NEURAL NETWORK AUGMENTATION OF ATTITUDE ESTIMATION USING NAVIGATION SATELLITE SIGNAL PHASE

R. Katoch[1]
Flt Cdr MCC, Air Force Station Ambala, Ambala Cantt 133001, India

P. R. Mahapatra[2]
Department of Aerospace Engineering,
Indian Institute of Science, Bangalore 560012, India

Abstract: Attitude estimation of an aircraft utilizing navigation satellite carrier phase measurements is studied. An Extended Kalman Filter (EKF) for the Euler angles is augmented by an artificial neural network (ANN) to improve its estimation performance. MLP and RBFN networks are trained for various levels of manoeuvre and measurement noise under complex manoeuvre scenarios. It is shown that the ANN provides significant improvement in the EKF performance. RBFN scores distinctly over MLP in terms of training time and estimation accuracy. The RBFN is optimized and the improvement through multipoint training is estimated.

Keywords: Neural networks, Extended Kalman filter, Attitude algorithms, Nonlinear systems, Satellite applications

1. INTRODUCTION

Navigation satellite systems such as GPS and GLONASS emit carrier signals with extremely stable and accurate frequency and phase. Measurements of differential phase of satellite signals between two or more spatially separated antennas mounted on a platform can be used to determine the attitude of the platform (Cohen *et al*., 1992; Lu *et al*., 1993). Determination of satellite attitude in space has been suggested using this method. However, attitude determination of aircraft is more challenging because of their higher dynamics, i.e., higher rates of manoeuvre.

Instantaneous measurements of satellite signal phase, and hence the vehicle attitudes derived from them, tend to be noisy. Because of the presence of nonlinearities, the extended Kalman filter (EKF) is employed at present to obtain optimal attitude estimates (Gelb, 1974; Zarchan, 2000). However, the EKF has certain limitations in terms of stability, adaptability and observability. It also requires perfect system and measurement models, and all noise processes to be white, Gaussian and known. Any violation of these assumptions results in degradation of the estimation accuracy, convergence rate and possibly failure of the filter.

Artificial neural networks (ANN) can 'learn' to map input-output relationships in a generic way, without specific *a priori* knowledge about them. Therefore a properly chosen neural network is capable of aiding the EKF to improve the accuracy of the attitude angle estimates after adequate training (Guanrong, 1994; Vaidehi *et al*., 2001; Vepa, 1993). This paper focuses on the effectiveness of neural networks of different types and complexities to improve the performance of the EKF for aircraft attitude estimation based on satellite signal phase measurement.

2. ATTITUDE DETERMINATION

The principle of attitude determination using satellite carrier phase measurements is shown in Fig. 1 (Ellis and Greswell, 1979). A master (M) and a slave (S) antenna separated by a baseline vector $\mathbf{a_B}$ (expressed in wavelengths) are mounted on a vehicle. The direction of the satellite with respect to the vehicle is denoted by the unit line-of-sight (LOS) vector $\mathbf{s_R}$. The satellite signal arrives at the closer antenna slightly before reaching the other. The differential propagation distance Δr between the antennas is the projection of $\mathbf{a_B}$ onto $\mathbf{s_R}$, which translates into a phase difference $\Delta\varphi$ at the carrier signal frequency. By measuring $\Delta\varphi$ a receiver can determine Δr. The measured phase difference $\Delta\varphi_m$ is written in terms of the unknown body attitude as

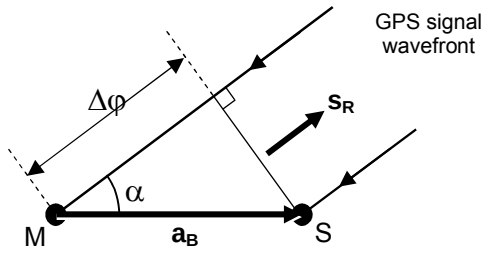

Fig.1 Geometry of single carrier phase difference

$$\Delta\varphi_m = (2\pi/\lambda)\mathbf{A_R^B}\ \mathbf{s_R}\cdot\mathbf{a_B} + \Delta\varphi_e \qquad (1)$$

where

$\mathbf{A}_{\mathbf{R}}^{\mathbf{B}}$ is a matrix representing the attitude of the body B with respect to the external reference frame R,
$\mathbf{s_R}$ is the sightline vector in the reference frame R,
$\mathbf{a_B}$ is the baseline vector in the body frame B,
$\Delta\varphi_m$ is the measured phase difference,
$\Delta\varphi_e$ is the unknown measurement error, and
λ is the satellite signal carrier wavelength.

The objective is to find the matrix $\mathbf{A}_{\mathbf{R}}^{\mathbf{B}}$, or its equivalent parameters in terms of the Euler angles or quaternions, from a set of phase difference measurements in Eq. (1).

3. FLIGHT SCENARIO AND MEASUREMENT SIMULATION

A case is considered in which four antennas mounted on an aircraft. Carrier phase measurements across three symmetric baselines ($\mathbf{a}_1$, $\mathbf{a}_2$, $\mathbf{a}_3$ in the plan view shown in Fig. 2) are utilized for attitude determination. The aircraft is simulated to 'fly' along pre-determined flight paths and its attitude is computed as a function of time. The expected phase differences of the carrier signal across the antenna baselines corresponding to these known attitude angles are computed with respect to two visible GPS satellites (Wu, 1998). To this, white Gaussian noise of known variance is added to simulate the measurements.

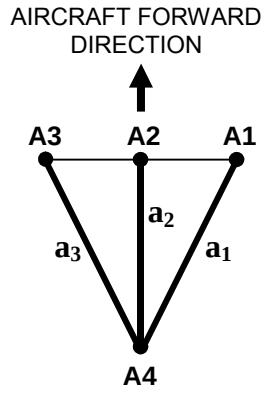

Antenna	Coordinates (m)
A1	(7.0,8.0,-2.5)
A2	(7.5,-0.124,-1.5)
A3	(7.0,-8.0,-2.5)
A4	(0.0,0.0,0.0)

Fig. 2 Antenna configuration

Using the above 'measurements', an EKF estimation of the attitude is performed, and compared with the known attitude angles in order to obtain the estimation error. The EKF is then augmented with an artificial neural network (ANN) which is first subjected to supervised learning by using the estimation error (of the stand-alone EKF) and filter gain as input parameters. Following the training phase, the ANN-EKF combination is switched over to the operating or 'test' mode wherein the ANN correction output is combined with the basic EKF output to yield the augmented output. The performance of the ANN-augmented EKF is evaluated by comparing the augmented output with the known attitude parameters.

The GPS satellite orbits and positions have been simulated using a software simulator. Aircraft simulations are based on a commercial/transport class, performing flight maneuvers under both training and test conditions. The flight paths have been simulated under the following conditions and assumptions:

(i) The aircraft flies at a constant speed of 200 m/s and a fixed altitude of 12,000 m

(ii) The flight path is achieved through roll and yaw maneuvers only

(iii) At constant flight speed and altitude, the pitch angle would remain constant; this is assumed zero without loss of generality

The matrix dynamical equation is derived from linearized attitude kinematics involving the three Euler angles (ψ,ϕ,θ):

$$\dot{\phi} = P + Q\sin\phi\tan\theta + R\cos\phi\tan\theta$$
$$\dot{\theta} = Q\cos\phi - R\sin\phi$$
$$\dot{\psi} = Q\sin\phi\sec\theta + R\cos\phi\sec\theta$$

where P, Q and R are the angular velocities of the aircraft about the body axis system.

The state vector $\mathbf{X}$ is the attitude vector $[\psi \quad \phi \quad \theta]^{\mathrm{T}}$. The transformation matrix is:

$$\mathbf{A}=\begin{bmatrix} \cos\theta\cos\psi & \sin\phi\sin\theta\cos\psi - \cos\phi\sin\psi & \cos\phi\sin\theta\cos\psi - \sin\phi\sin\psi \\ \cos\theta\sin\psi & \sin\phi\sin\theta\sin\psi + \cos\phi\cos\psi & \cos\phi\sin\theta\sin\psi + \sin\phi\cos\psi \\ \sin\theta & \sin\phi\cos\theta & \cos\phi\cos\theta \end{bmatrix}$$

4. FLIGHT PROFILES

Three flight profiles are considered in this study: (1) circular maneuver (Fig. 3) of varying radii, simulating various bank angles both clockwise and anticlockwise motion, (2) double-loop or 'figure-of-eight' path (Fig. 4), also called 'roll-doublet', and (3) laterally undulating path composed of semicircular segments of decreasing radius, i.e. increasing maneuver (Fig. 5).

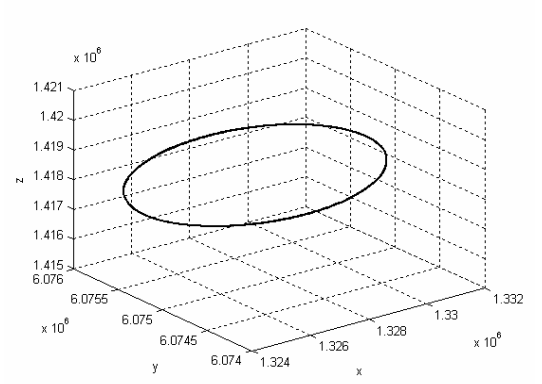

Fig. 3 Circular flight path

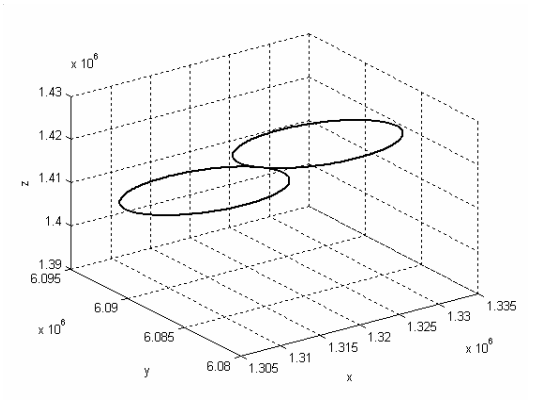

Fig. 4 Double-loop (figure-of-eight) flight path

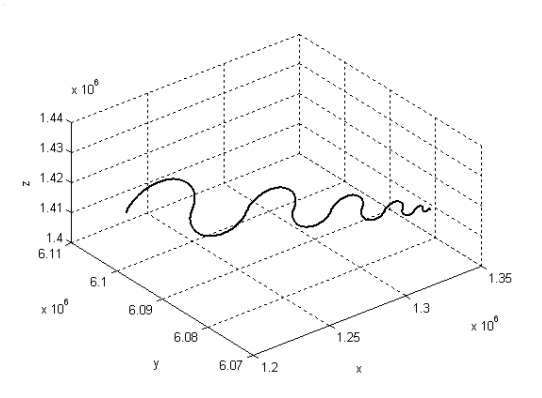

Fig. 5 Laterally undulating flight path

5. ANN AIDING OF EKF

Both Radial Basis Function (RBF) and Multilayer Perceptron (MLP) types of ANN with varying complexities (number of neurons) have been studied in the context of attitude determination.

5.1 MLP Network

The MLP is a popular neural network employed for varied problem solving using supervised learning through the error back-propagation algorithm (Haykin, 2005). The standard delta rule is used to update the weights of the network:

$$\Delta W_{ji}^{s}(t) = \eta e_j^s(t) u_i^{s-1}(t) + \beta \Delta W_{ji}^{s}(t-1)$$

where η is the learning coefficient; ΔW_{ji}^{s} is the change of weight between the i^{th} neuron in layer (s–1) and the j^{th} neuron in layer (s) at time t. e_j^s is the error (difference between desired and actual values) of the j^{th} neuron in layer (s) at time t. β is the momentum coefficient and u_i^{s-1} is the output of the i^{th} neuron in the $(s-1)^{\text{th}}$ layer at time t. The MLP network employed was optimized 2 hidden layers, each with 50 nodes.

5.2 RBF Networks

These networks are designed as a curve fitting (approximation) problem [15]. It involves three layers, which include the input, the output, and the hidden layer. The hidden layer applies a nonlinear transformation from the input space to the output space. The following Green's function has been used as the activation function of the hidden i^{th} neuron:

$$\phi(x_t, c_i, \sigma_i) = \exp(-\|x_t - c_i\|^2 / (2\sigma_i^2 \times h))$$

where x_t is the input, c_i is center, σ_I is the radius (or width), and h is the overlap parameter. The RBF network (RBFN) was optimized for 200 neurons and an overlap parameter of 25.

5.3 Network Architecture

ANN aiding of EKF is carried out in two phases: training and operation (Simon, 2001; Fisher and Rauch, 1994). The architecture for the training phase is shown in Fig. 6 wherein the ANN may be either an MLP or an RBF network. The training is carried out using nine input signals:

1. Three differences between the true values $\mathbf{X}=(\psi_t,\varphi_t,\theta_t)$ of Euler angles and the values $\mathbf{X}_{\text{kp}}=(\psi_p,\varphi_p,\theta_p)$ estimated by EKF
2. Three differences between the predicted Euler angles $\mathbf{X}_{\text{km}}=(\psi_m,\varphi_m,\theta_m)$ and $\mathbf{X}_{\text{kp}}$ estimated by the EKF
3. Three Kalman gains ($K1$, $K2$, $K3$) of the respective Euler angles.

The true attitude angles as well as the error quantities used for supervised training are known during the simulation process.

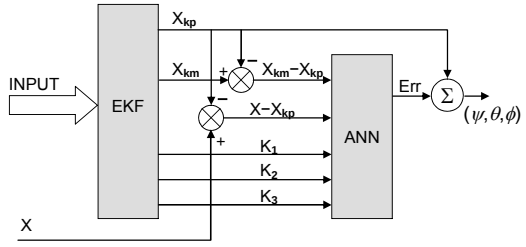

Fig. 6 Configuration of ANN aided EKF in the training mode

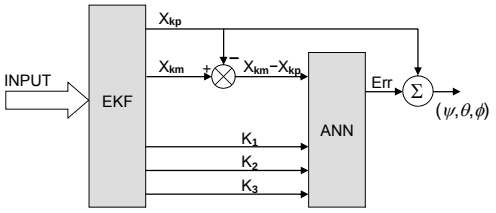

Fig. 7 Configuration of ANN aided EKF in the test/operating mode

In the operating or 'test' phase, the true values of the state vector **X** are not known. Hence the ANN-EKF utilizes only 6 inputs as shown in Fig. 7.

6. RESULTS

Two cases were considered for the study, one focusing on maneuver and the other on measurement noise levels.

6.1 Case I

The ANN here was trained for roll angle variations in a circular pattern (Fig. 3) and then the ANN-EKF performance was tested for the two test maneuvers shown in Figs. 4 and 5. The phase measurement noise was held constant at 4° for this study. The RBFN was found to train much faster (average 23.433 s) than the MLP (53.548 s). The percentage reduction in estimation error due to ANN aiding of EKF over the stand-alone EKF is shown in Table 1 for the training phase and in Table 2 for the operational phase. It is evident that the RBFN offers distinctly better estimation accuracy than the MLP. Therefore only figures comparing the RBFN aided EKF with the stand-alone EKF are presented below.

Table 1 Improvement in EKF attitude estimate with ANN aiding during training

Roll angle in training (Deg)	Improvement with MLP aiding EKF (%)			Improvement with RBFN aiding EKF (%)		
	ψ	ϕ	θ	ψ	ϕ	θ
11.0	15.0	5.3	9.15	57.0	46.11	43.9
16.7	2.16	0.68	6.56	66.8	31.86	45.48
26.7	2.7	1.92	8.98	61.56	38.97	44.2
30.74	0.92	4.12	0.8	62.81	41.13	46.41
38.3	1.79	0.64	0.93	66.7	47.82	54.68
-26.7	6.1	6.8	13.5	69.12	40.44	40.17
-30.74	6.3	8.64	11.7	56.89	33.07	32.71
-38.3	2.6	20.7	14.2	59.36	45.52	43.26

Table 2 Improvement in EKF attitude estimate with ANN aiding during operation

Test Maneuver	Improvement with MLP aiding EKF, %			Improvement with RBFN aiding EKF, %		
	ψ	ϕ	θ	ψ	ϕ	θ
Double-loop	4.06	6.87	10.7	81.05	50.56	72.31
Undulating	1.48	2.14	6.42	40.21	47.79	43.09

The double-loop maneuver of Fig. 4 involves a bank angle of ±26.59°, thereby testing the network capability within its training bounds (±38.3°). To test the ANN beyond the training bounds, the undulating flight path of Fig. 5 is used, with bank angles over segments varying up to 45°. Table 2 shows that operation within the training bounds leads to better performance of the ANN-EKF compared to operation outside the bounds.

Fig. 8 shows the plots of error in attitude angles for the lateral undulating flight path maneuver for the stand-alone EKF. The RMS errors in Euler angles over the flight time were: ψ = 0.5036°, ϕ = 0.5907° and θ = 0.8137°. The corresponding errors for ANN-EKF are plotted in Fig. 9, with RMS values: ψ = 0.301°, ϕ = 0.292° and θ =0.463°.

6.2 Case II

Here the ANN was trained for varying levels of measurement noise, using a double-loop maneuver with bank angle of ±26.59°. The percentage reduction in estimation error due to RBFN aiding of EKF over the stand-alone EKF during training is seen from the measurement errors in Table 3.

Table 3 Improvement in EKF attitude estimate with ANN aiding for varying noise levels during training

Phase Measurement Noise (Deg)	Improvement with RBFN aiding EKF, %		
	ψ	ϕ	θ
5	78.6	39.19	65.20
10	62.68	45.42	40.79
20	48.94	39.28	38.84
30	42.28	40.48	39.02
35	51.81	40.08	30.75
40	47.06	40.65	38.19

The performance of the stand-alone EKF shows strong degradation with increase in measurement noise. During the operational phase the network was subjected to measurement noise of 15°. The errors for the stand-alone EKF and the RBFN-aided EKF are shown in Figs. 10 and 11 respectively. The RMS errors for the two cases and the percentage improvement achieved by RBFN aiding are listed in Table 4.

Table 4 Improvement in EKF attitude estimate with ANN aiding during operation with 15° phase noise

Estimator	ψ (Deg)	ϕ (Deg)	θ (Deg)
EKF alone	1.28	2.79	0.7553
RBFN-EKF	0.64	1.81	0.48
% Improvement	50.18	35.34	35.42

7. CONCLUSIONS

A comparative study has been made between a conventional EKF and an ANN-aided EKF in performing aircraft attitude estimation using differential measurements of the carrier phase of GPS signals. Optimum MLP and RBF networks have been studied for their ability to augment EKF for various maneuver and measurement noise levels.

The overall performance of the ANN aided EKF is markedly superior to that of the stand-alone EKF for a wide range of operating conditions and error inputs. Between the two classes of ANNs, RBFN is found to score over the MLP network in terms of system complexity, training speed and estimation accuracy. Once the training is imparted to the ANN, the operation is quite straightforward, permitting real-time implementation even for aerospace applications. This can also be used for improving the performance of medium- and low-accuracy GPS attitude sensing applications.

The ANN is able to improve the EKF performance by compensating for unmodeled states and biases, and probably benefits from the constraints imposed on EKF by its assumptions.

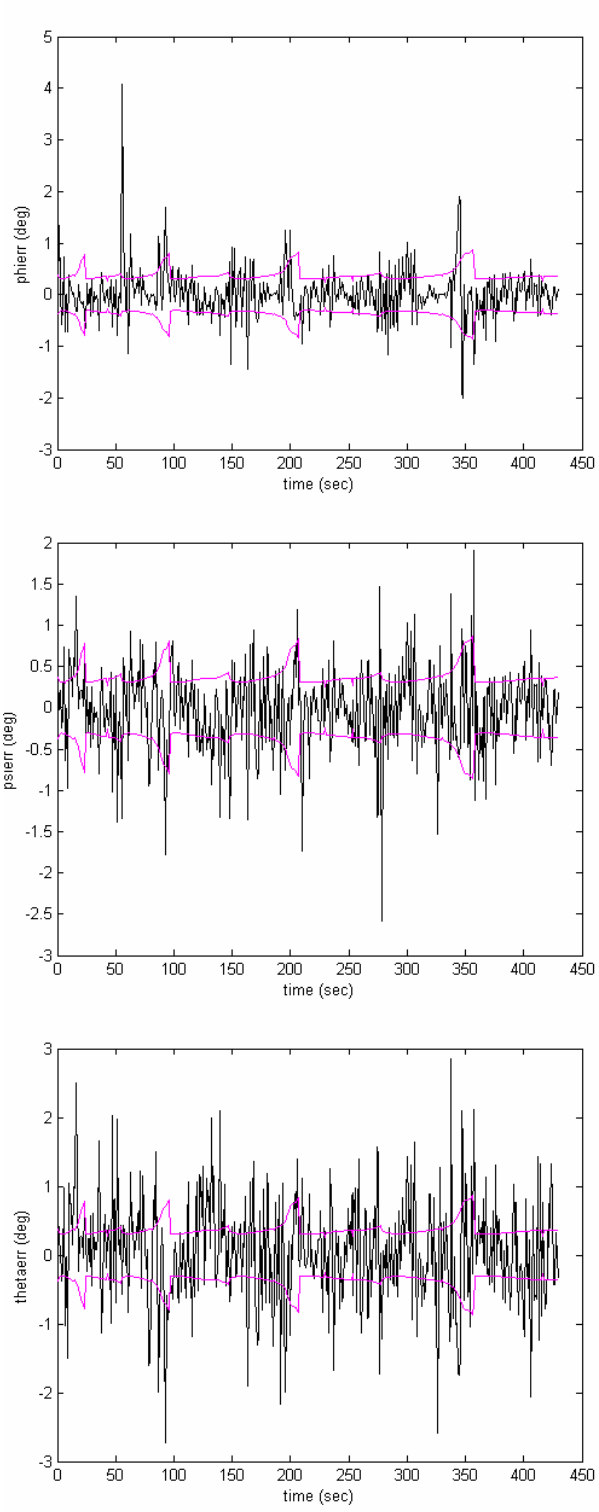

Fig 8 Error in attitude angles for stand-alone EKF for lateral undulating maneuver of Fig. 5

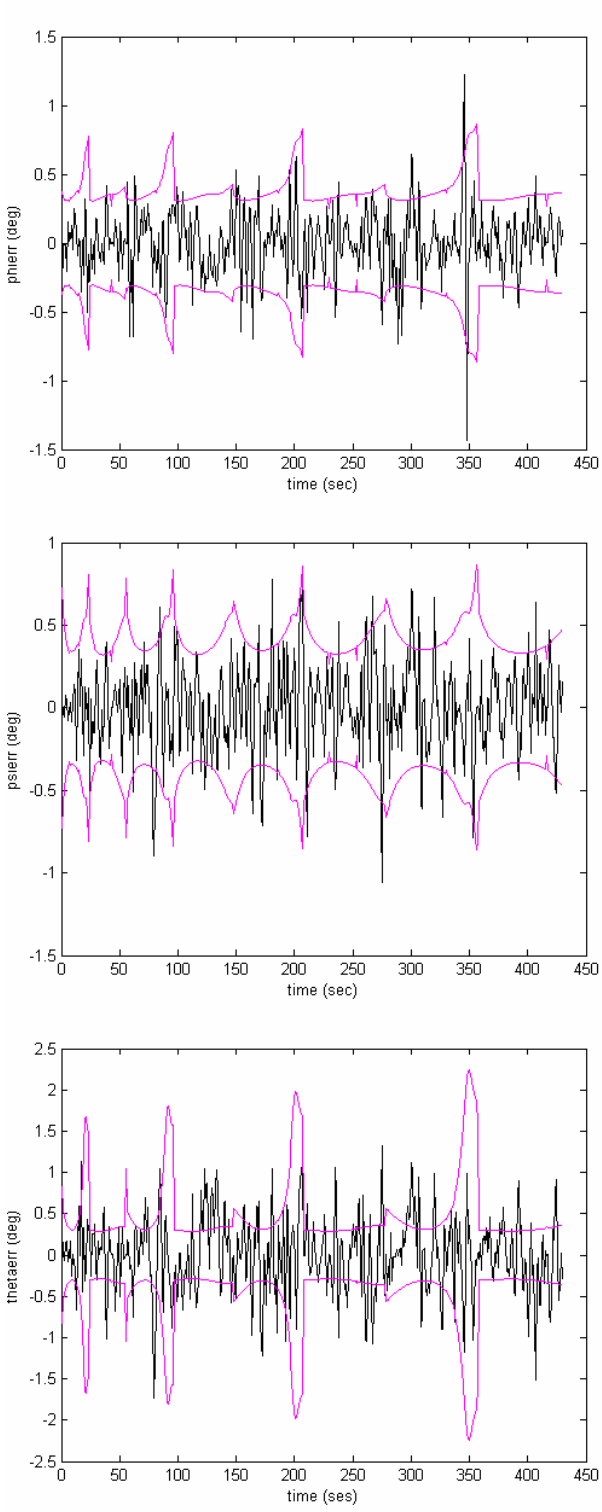

Fig 9 Error in attitude angles for RBFN-aided EKF for lateral undulating maneuver of Fig. 5

REFERENCES

Cohen, C.E. and B.W. Parkinson (1992). Aircraft applications of GPS based attitude determination. *Proc. 5th International Technical Meeting of the Satellite Division of the ION,* GPS-92, Albuquerque, NM.

Ellis, J.F. and G.A. Greswell (1979). Interferometric Attitude Determination with the Global Positioning System, *Journal of Guidance and Control*, **12**, 523-527.

Fisher, W.A. and H.E. Rauch (1994). Augmentation of extended Kalman filter with a neural network. *Proc. IEEE International Conference on Neural Networks,* Orlando, Florida, 1191-1196.

Gelb, A. (1974). *Applied Optimal Estimation*. MIT Press, Cambridge, MA.

Guanrong, C. (1994). Application of neural networks in target tracking data fusion. *IEEE Trans. Aerospace and Electronic Systems*, **30**, 281-287.

Haykin, S. (2005). *Neural Networks: A Comprehensive Foundation*. Pearson Prentice Hall.

Lu, G., M.E. Cannon and G. Lachapelle (1993). Attitude determination in a survey launch using multi-antenna GPS technologies. *National*

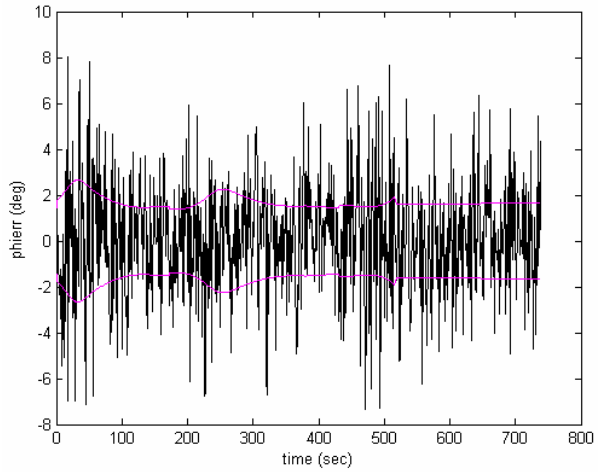

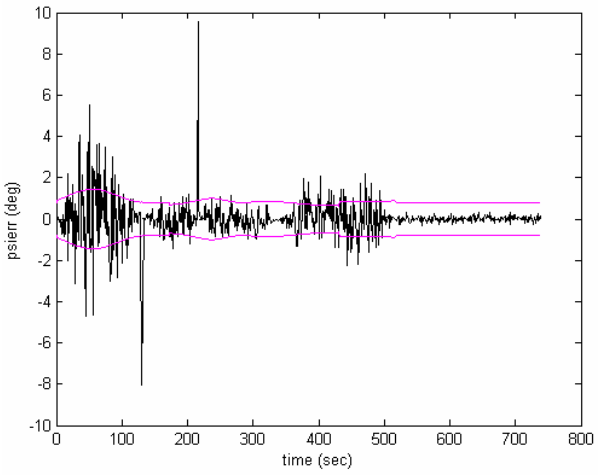

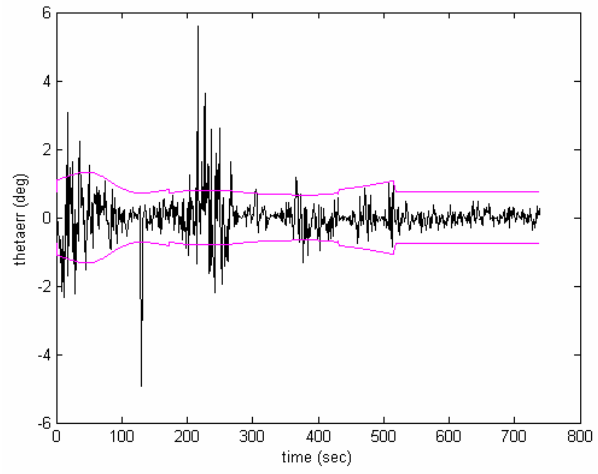

Fig 10 Error in attitude angles for stand-alone EKF for phase measurement noise of 15^0

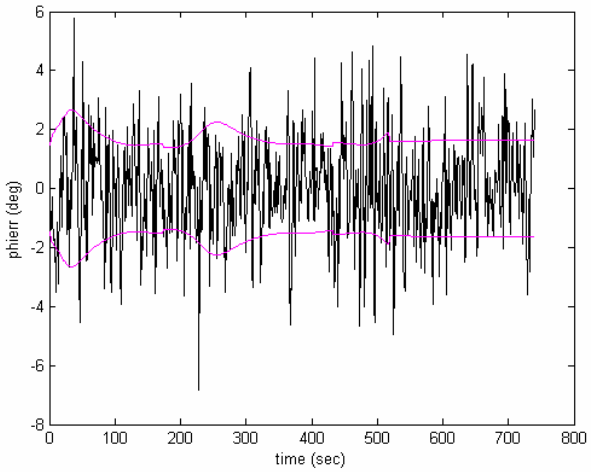

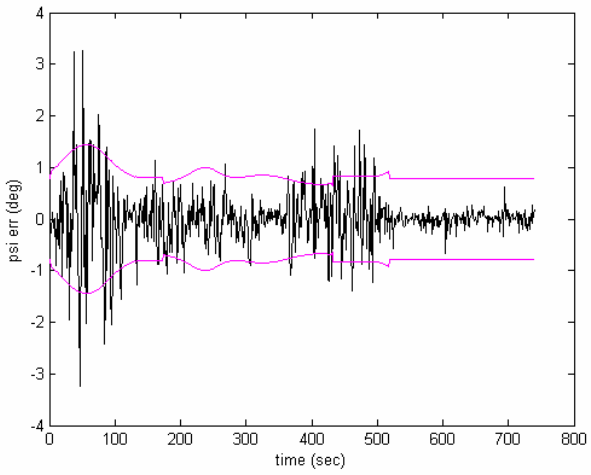

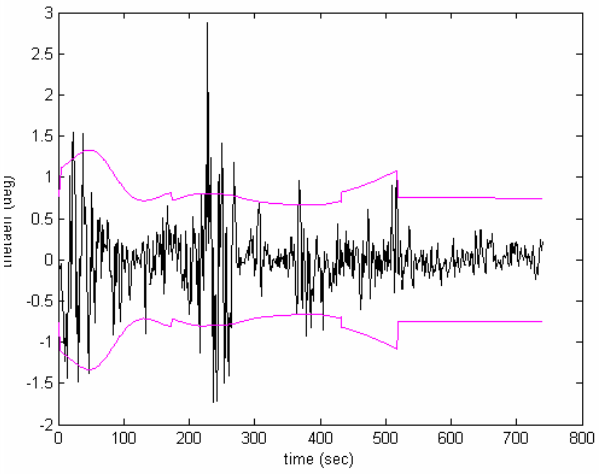

Fig 11 Error in attitude angles for RBFN-aided EKF for phase measurement noise of 15^0

Technical Meeting, Institute of Navigation, San Francisco, 20-22.

Simon, D. (2002). Training radial basis neural networks with the extended Kalman Filter. *Neurocomputing*, **48**, 455-475.

Vaidehi, V., N. Chitra, C.N. Krishnan and M., Chokkalingam (2001). Neural network aided Kalman filtering for multitarget tracking applications. *International Journal of Computers and Electrical Engineering*, **27**, 217-228.

Vepa, R (1993). Application of neuro Kalman filtering to attitude estimation of platforms and space vehicles. *IEE Colloquium on High Accuracy Platform Control in Space*, 5/1-5/3.

Wu, J., W. Zheng and Z. Jianhua (1998). Attitude determination using two satellites of Global Positioning System. *AIAA Guidance, Navigation, and Control Conference and Exhibit*, Boston, MA, 1940-1944.

Zarchan, P. and H. Musoff (2000). *Fundamentals of Kalman Filtering: A Practical Approach*. *Progress in Astronautics and Aeronautics*, **190,** American Institute of Aeronautics and Astronautics.